Building Tomorrow's Society
Bâtir la Société de Demain

Fredericton, Canada
June 13 – June 16, 2018/ *Juin 13 – Juin 16, 2018*

FRP REINFORCED GLULAM BEAMS UNDER HIGH STRAIN-RATES

Lacroix, Daniel[1,3] and Doudak, Ghasan[2]
[1] Carleton University, Canada
[2] University of Ottawa, Canada
[3] Daniel.Lacroix2@Carleton.ca

Abstract: An experimental program investigating the potential for using fibre-reinforced polymers (FRP) as a strengthening option for glulam beams subjected to simulated blast loads was undertaken. A total of seven different retrofit configurations were investigated. Increases in resistance and maximum deflection at peak resistance in the range of 1.35-1.57 and 1.30-1.62, respectively, were obtained when FRP tension laminates with and without confinement were used. The addition of FRP confinement prevented premature de-bonding and significantly altered the failure mode from simple or splintering tension failure to a combination of brash tension and compression failure while limiting the damage to a small region. Whereas the use of unidirectional FRP as confinement did not contribute significantly to the post-peak resistance, the use of bidirectional FRP significantly improved the post-peak resistance above the 50% threshold for deflections corresponding to 1.57-3.40 that recorded at peak resistance.

1 INTRODUCTION

The increased presence of glulam in high-profile structures may put them at risk for deliberate attacks or accidental explosions. The available literature on the behaviour of glulam under such loading is scarce (e.g. Lacroix 2017). Also, while design guidelines in the Canadian blast standard (CSA 2012) exist on the strengthening and retrofitting of structural elements using fibre-reinforced composite materials for reinforced concrete and masonry, such provisions are lacking for wood elements. However, significant research has been conducted on the behaviour of retrofitted wood members under static loading.

Research conducted on the behaviour of FRP reinforced wood members under static loading have shown that increases in resistance and stiffness for wood reinforced with simple FRP tension reinforcement of up to 50% and 20%, respectively, can be attained (Buell and Saadatmanesh 2005, Hernandez et al. 1997, Johns and Lacroix 2000, Yang et al. 2016). It is important to note that these increases highly depend on the type and amount of reinforcement provided, reinforcement scheme (e.g. horizontal or vertical, sheets or bars), and type of wood tested (i.e. lumber, timber, EWP).

The main drawback in using simple tension reinforcement is the accompanied partial- or full-length de-bonding of the reinforcement when the outer wood tension layers fail (Dorey and Cheng 1996a, Dorey and Cheng 1996b, Hernandez et al. 1997). Buell and Saadatmanesh (2005) investigated the effect of wrapping timber beams with carbon FRP (CFRP), which was found to provide confinement to the wood, and thereby reducing the effects of defects. Johns and Lacroix (2000) investigated the effect of simple longitudinal tension reinforcement and half U-shaped longitudinal reinforcement on sawn lumber. It was observed that the presence of FRP material arrested the crack opening, confined local rupture, and bridged local defects naturally found in wood. Sonti et al. (1996) investigated the effect of partial-length reinforcement and found

that providing such confinement enhanced the strength and stiffness in the order of 2.1 to 23.2% and 1.9 to 9.3%, respectively.

The current paper is part of a broader research program investigating the behaviour of glulam beams and columns subjected to simulated blast loadings (Lacroix 2017). Herein presented are some key experimental results of the test program involving the flexural retrofit of full-scale glulam beams using both unidirectional and bidirectional glass FRP (GFRP). Full-scale retrofitted beams were tested destructively under both static and dynamic loading.

2 EXPERIMENTAL PROGRAM

2.1 Description of Specimens

A total of sixteen 137 x 222 mm^2 24f-ES Spruce-Pine retrofitted glulam beams were tested to failure under simply supported static and dynamic four-point bending. The glulam layup consisted of six laminates in width and five laminates in depth and was manufactured according to ASTM D3737 (ASTM 2012) to meet the specifications of CSA O177 in Canada (2015). A total of seven different GFRP retrofit configurations, used to enhance the flexural behaviour of the beams were investigated. The experimental program involved investigating the effects of unidirectional and multi-directional fabrics on the post-peak behaviour of the beams. The test matrix for both the unretrofitted and retrofitted beams is presented in Table 1.

Table 1: Test matrix

Specimen type	Loading type	Specimens	FRP retrofit configuration
Unretrofitted	Static	B1-B4	-
	Dynamic	B5-B9	-
Retrofitted	Static	R1-1, R1-2	T[0]2
	Dynamic	R1-3, R1-4	T[0]2
	Static	R2-1, R2-2	T[0]2C[90]
	Dynamic	R2-3, R2-4	T[0]2C[90]
	Static	R3-1, R3-2	U[0]2C[90]
	Dynamic	R3-3, R3-4	U[0]2C[90]
	Dynamic	R4-A	U[0]2C[0/90]2
	Dynamic	R4-B	C[0/90]4
	Dynamic	R5-A	U[0]2C[±45]2
	Dynamic	R5-B	C[±45]4

Specimens are identified with letters B, or R, denoting whether the specimen is an unretrofitted beam, or retrofitted beam, respectively. For the retrofitted specimens, the stacking sequence is presented in terms of simple tension reinforcement (T) or U-shaped tension reinforcement (U) and confinement (C). Found in the square brackets is the fibre orientation of the fabric used while the subscript denotes the number of layers applied in cases where there were multiple layers applied.

Retrofit 1 consisted of two layers of GFRP tension reinforcement. Due to the known issue of de-bonding of the FRP reinforcement, a layer of unidirectional GFRP in the perpendicular to wood fibre direction was added in Retrofit 2. Investigated in Retrofit 3 is the effect of a tension U-shaped GFRP with partial-length confinement. Retrofit 4-A consisted of two unidirectional GFRP U-shaped layers along with two layers of 0/90 bidirectional GFRP whereas Retrofit 4-B consisted of four layers of 0/90 bidirectional GFRP. Similarly, Retrofit 5-A consisted of two unidirectional GFRP U-shaped layers along with two layers of ±45 bidirectional GFRP whereas Retrofit 5-B consisted of four layers of ±45 bidirectional GFRP. For both Retrofits 4 and 5, the reinforcement was applied in the direction parallel to the length of the beam such that the reinforcement on the tension side was continuous.

2.2 Static and Dynamic Test Setups

To establish the flexural behaviour of the specimens, static and dynamic four-point bending tests with simply supported boundary conditions and a clear span of 2,235 mm were conducted. Figure 1 shows the static and dynamic test setups where it can be seen that the same loading pattern, span, and boundary conditions were used to allow for a direct comparison between the two loading regimes.

(a) Static (b) Dynamic

Figure 1: Test setups

Data acquisition systems with sampling rates of 10 and 100,000 samples per second for the static and dynamic tests, respectively, were used to record the beams' response. Reactions, mid-span displacement, and tensile and compressive strain-time histories were recorded for the static tests. Similarly, the reflected pressure, mid-span displacement, reactions, and mid-span tensile and compressive strain-times histories were measured for the dynamic tests.

3 EXPERIMENTAL RESULTS AND ANALYSIS

3.1 Characterization of Failure Modes

Representative static and dynamic failure modes for Retrofits 1 through 3 are shown in Figure 2. Both the static (Fig. 2a) and dynamic (Fig. 2d) failure of Retrofit 1 was characterized by a failure in the outer wood tension laminates with extensive damage throughout the depth of the cross-section. Upon initial wood tensile failure, the outer tension laminates pushed outwards on the GFRP causing separation between the wood and reinforcement. The overall failure of the wood was dominated by simple or splintering tension failure that was influenced by the presence of knots or finger-joints.

(a) R1-1

(b) R2-1

(c) R3-1

(d) R1-4

(e) R2-4

(f) R3-3

Figure 2: Representative static and dynamic failure modes for Retrofits 1 through 3

The failure mode observed in Retrofit 2 significantly differed from that observed in Retrofit 1. A brash tension failure resulting in a straight cut through the beam width was observed under both static (Fig. 2b) and dynamic (Fig. 2e) loading. The addition of full-length confinement prevented the separation between the tension GFRP reinforcement and the wood tension face while also limiting the damage to the wood to a small section with significant compression failure. Furthermore, as anticipated in unidirectional FRP fabric, tearing in the FRP confinement perpendicular to the fibre direction was observed (Figs. 2b and 2e).

Representative static and dynamic failures for Retrofit 3 are shown in Figures 2c and 2f, respectively. While some separation of the FRP tension reinforcement was observed (Figs. 2c and 2f), it occurred at a deflection level that was beyond that obtained at peak resistance. The specimens investigated in Retrofit 3 were able to maintain some level of post-peak resistance. For example, specimen R3-3 deflected approximately 1.6 times more than the deflection corresponding to peak resistance without de-bonding of the FRP.

Figure 3a shows the final deflected shape of specimen R4-A, where the de-bonding occurred past the point of ultimate resistance. Specimen R4-B, which deflected to a maximum displacement corresponding to 4.15 times that recorded at peak resistance without any de-bonding, is shown in Figure 3b. While specimen R4-B did not reach complete failure (i.e. blowout) and recovered part of its displacement, local “buckling” of the FRP on the compression face near the mid-span region was observed. Specimen R5-A, shown in Figure 3c, was subjected to a pressure-impulse combination similar to that of specimen R4-A, and as it can be seen the permanent deflection as well as the associated damage in R5-A is significantly less. While Specimen R5-A did not reach ultimate failure, it recovered with a permanent deflection corresponding to sixty percent of the maximum displacement. Specimen R5-B (Figure 3d) was subjected to a pressure and

impulse combination similar to that specimen R5-A was exposed to. The specimen deflected 3.6 times that recorded at peak resistance.

(a) R4-A (b) R4-B (c) R5-A (d) R5-B

Figure 3: Representative static and dynamic failure modes for Retrofits 4 and 5

3.2 Analysis of Experimental Test Results

3.2.1 Static

The key static test results for the retrofitted beams are presented in Table 2 along with the average of the unretrofitted beams obtained from previous work conducted by the authors (Lacroix 2017).

Figure 4 shows the static resistance curves for the retrofitted specimens as well as the average of the unretrofitted beams. Providing two layers of GFRP tension reinforcement (e.g. Retrofit 1) increased the ultimate resistance by a factor of 1.35, deflection at ultimate resistance by a factor of 1.30, and stiffness by a factor of 1.1 compared to the unretrofitted beams. Although the reinforcement enhanced the stiffness and strength of the beam on average, it did not provide significant post-peak resistance. The addition of GFRP confinement in addition to the tension reinforcement (e.g. Retrofit 2) increased the ultimate resistance, deflection at ultimate resistance, and stiffness by factors of 1.40, 1.39, and 1.13 relative to the unretrofitted beams, respectively.

Table 2: Static test results

Specimen	R_{max}[a] (kN)	Δ_{Rmax}[b] (mm)	K[c] (kN/mm)	$\varepsilon_{t,w\text{-}f}$[d] x 10^{-4} (mm/mm)	$\varepsilon_{t,w\text{-}sf}$[e] x 10^{-4} (mm/mm)	$\varepsilon_{t,FRP\text{-}f}$[f] x$10^{-4}$ (mm/mm)	$\varepsilon_{c,w\text{-}f}$[g] x 10^{-4} (mm/mm)
B_{AVG}	*141.6*	*23.7*	*6.0*	*40.8*	-	-	*-52.4*
R1-1	196.7	32.9	6.4	39.2	37.5	40.2	-42.0
R1-2	186.2	28.9	6.7	40.8	28.0	41.8	-37.8
$R1_{AVG}$	*191.5*	*30.9*	*6.6*	*40.0*	*32.7*	*41.0*	*-39.9*
R2-1	206.3	32.6	6.7	44.1	37.6	45.1	-47.3
R2-2	189.8	33.2	6.8	49.0	35.0	51.4	-94.5
$R2_{AVG}$	*198.0*	*32.9*	*6.8*	*46.5*	*36.3*	*48.2*	*-70.9*
R3-1	214.3	38.5	6.6	43.6	-	94.2	-60.7
R3-2	230.3	38.6	6.8	48.3	33.8	50.2	-
$R3_{AVG}$	*222.3*	*38.5*	*6.7*	*46.0*	*33.8*	*72.2*	*-60.7*

[a] Maximum (peak) resistance

[b] Deflection at peak resistance

[c] Stiffness

[d] Strain at tensile rupture on tension face

[e] Strain at tensile rupture at 21 mm from tension face

[f] FRP maximum strain

[g] Maximum wood compressive strain

The confinement provided some post-peak resistance, albeit small in comparison to peak resistance. Retrofit 3 had a significant post-peak resistance (Fig. 4) of approximately 75% of the ultimate resistance. Retrofit 3 provided increases of 1.57, 1.62, and 1.12 in resistance, deflection at peak resistance, and stiffness, respectively, when compared to the unretrofitted beams.

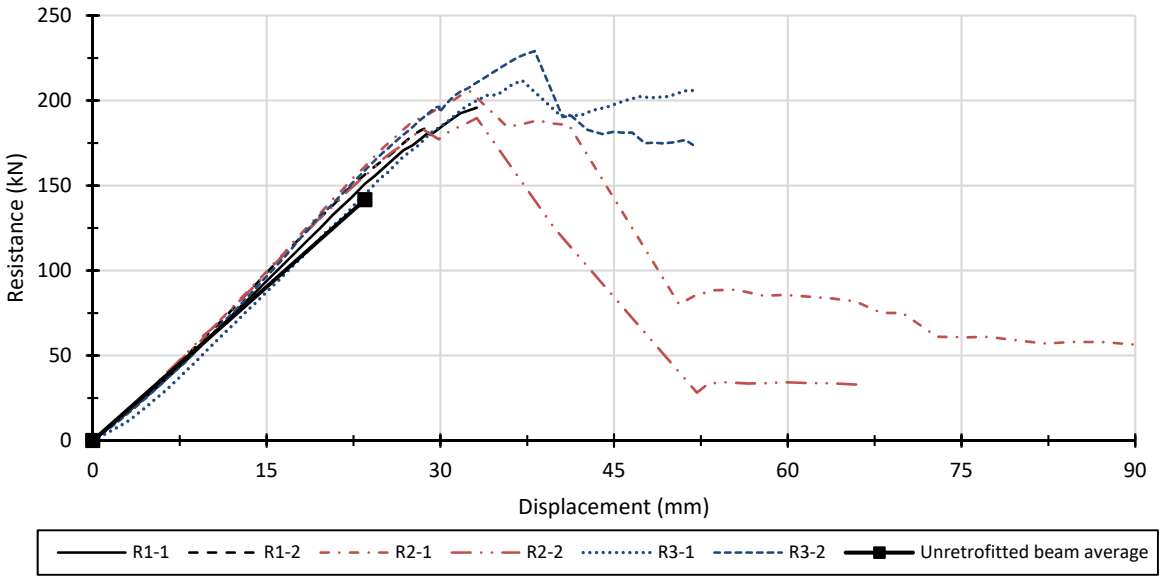

Figure 4: Static resistance curves of retrofitted beams compared to unretrofitted beam average

3.2.2 Dynamic

The key dynamic test results are summarized in Table 3 along with the results of the dynamically tested unretrofitted beams.

Table 3: Dynamic test results

Specimen	P_R[a] (kPa)	I_R[b] (kPa-ms)	R_{max-d}[c] (kN)	Δ_{Rmax}[d] (mm)	K[e] (kN/mm)	ε_{f-T}[f] x 10^{-4} (mm/mm)	ε_{f-Ts}[g] x 10^{-4} (mm/mm)	ε_{f-FRP}[h] x 10^{-4} (mm/mm)	ε_{f-C}[i] x 10^{-4} (mm/mm)
B_{AVG}	53.0	561	153.6	28.4	5.9	37.6	-	-	-47.4
R1-3.1	52.2	577	156.1	26.7	6.9	39.5	32.5	88.9	-37.2
R1-4.1	68.7	727	216.1	36.9	6	49.1	40.5	51.9	-41.4
R2-3.1	62.3	718	198.0	32.7	6.0	42.8	34.7	61.1	-133.1
R2-4.1	68.8	757	208.0	34.6	6.0	N/A[j]	N/A[j]	N/A[j]	N/A[j]
R3-3.1	63.5	698	213.0	40.3	6.4	51.8	N/A	175.3	-113.9
R3-3.2	73.8	829	183.7	61.0	3.0	N/A[j]	N/A[j]	165.9	-73.6
R3-4.1	67.6	818	242.3	41.7	6.5	49.8	33.8	118.6	N/A[j]
R3-4.2	74.4	780	182.9	58.9	3.5	N/A[j]	N/A[j]	113.4	N/A[j]
R4-A	76.3	1,091	241.2	38.2	6.3	42.8	-	143.9	-164.3
R4-B	71.5	1,092	242.9	37.7	6.5	45.5	-	207.8	-69.9
R5-A	74.6	1,153	246.0	36.0	7.4	43.2	-	152.7	-54.7
R5-B	65.7	1,170	234.3	38.9	6.4	47.7	-	251.0	-59.7

[a] Reflected pressure

[b] Reflected impulse

[c] Beam dynamic resistance

[d] Deflection at peak resistance

[e] Stiffness

[f] Strain at tensile rupture on tension face

[g] *Strain at tensile rupture at 21 mm from tension face*

[h] FRP maximum strain

[i] Maximum wood compressive strain

[j] Strain gauge malfunction

A comparison of the dynamic resistance of Retrofits 1 to 3 (Table 3) to the static average of its respective retrofit (Table 2) shows an average increase of 1.15. The dynamic resistance was obtained by considering the dynamic equilibrium of the system using a single-degree-of-freedom approach (Lacroix 2017), The apparent increase in strength is associated with high strain-rate effects. The dynamic increase factor (DIF) obtained in this study compares well with the value of 1.14 found in the literature based on comparison between static and dynamic resistance of unretrofitted glulam beams (Lacroix 2017).

Figure 5 shows the dynamic resistance curves of the retrofitted specimens where it can be seen that in general significantly greater deflections were experienced by the specimens during the dynamic testing compared to the static testing.

From Table 3 and Figure 5, it can be seen that the various configurations of reinforcement provided similar peak resistance (R_{max}), but different post-peak behaviour. While the addition of confinement for Retrofits 2 and 3 improved the post-peak resistance in comparison to the unretrofitted beams and Retrofit 1 beams, the use of multi-directional fabric significantly improved the post-peak behaviour. Post-peak resistance,

above the 50% threshold of peak resistance, was sustained for deflections ranging between 1.57 and 3.40 that recorded at peak resistance for Retrofits 4 and 5.

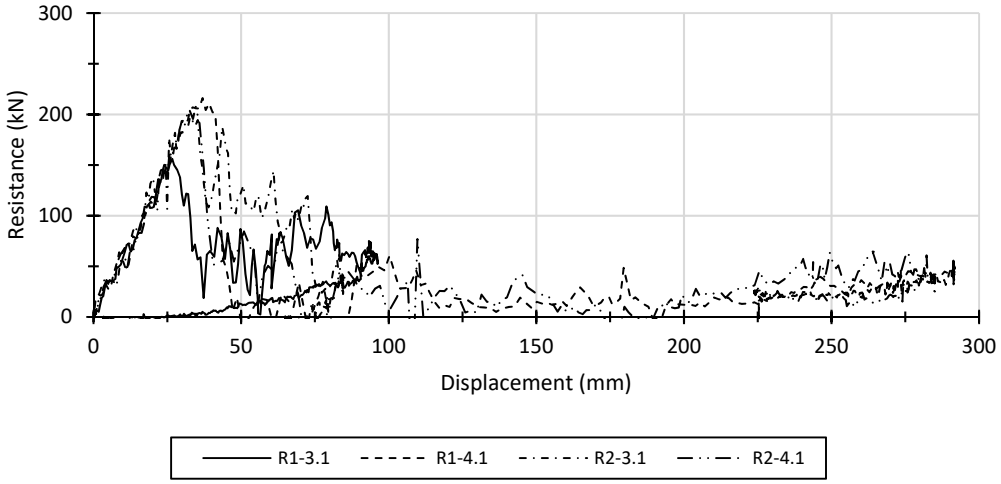

(a) Retrofits 1 and 2

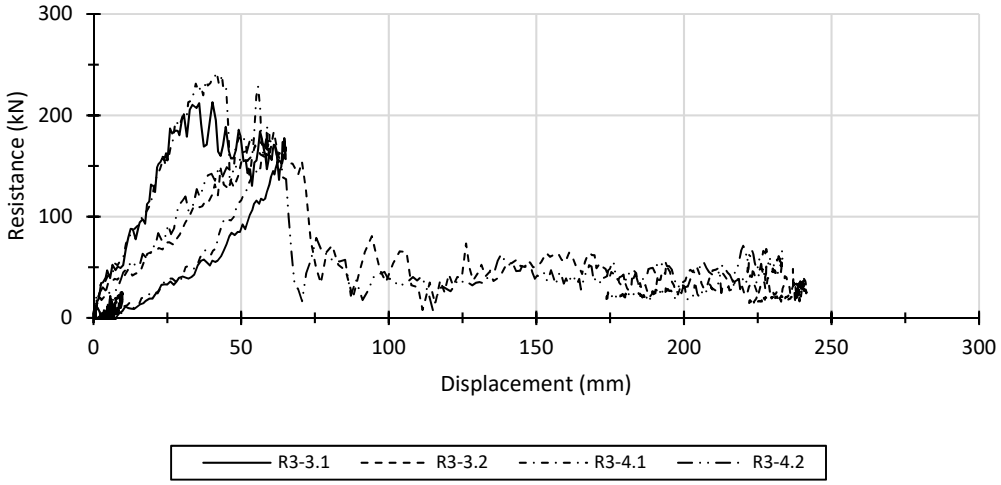

(b) Retrofit 3

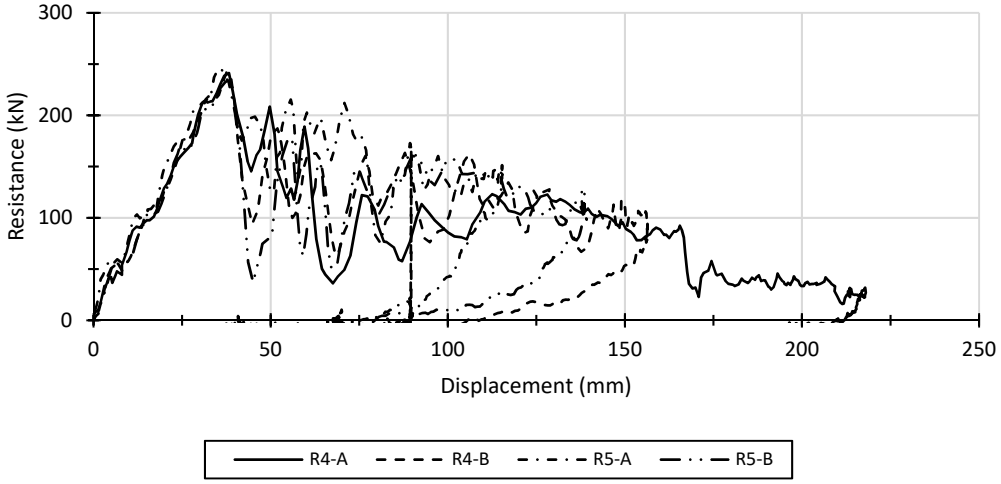

(c) Retrofits 4 and 5

Figure 5 Dynamic resistance curves of retrofitted beams

4 CONCLUSIONS

Results from an experimental program investigating the behaviour of retrofitted glulam beams using unidirectional and bidirectional FRP were presented. Increases in resistance and deflection at peak resistance in the order of 1.35-1.57 and 1.30-1.62, respectively, were observed for the reinforced beams relative to the unretrofitted beams. While adding simple tension reinforcement contributed to an increase in performance, this retrofit resulted in premature de-bonding between the FRP and the wood. Adding confinement prevented premature de-bonding and significantly altered the failure mode from simple or splintering tension failure to a combination of brash tension and compression failure while limiting the damage to a small region. Apart from Retrofit 3, none of the retrofit configurations investigated using unidirectional FRP significantly contributed to the post-peak behaviour. The use of bidirectional FRP in Retrofits 4 and 5 significantly increased the post-peak behaviour.

References

ASTM. 2012. Standard Practice for Establishing Allowable Properties for Structural Glued Laminated Timber. *ASTM D3737-12*. West Conshohocken, PA, ASTM International.

Buell, T.W., and Saadatmanesh, H. 2005. Strengthening timber bridge beams using carbon fiber. *Journal of Structural Engineering*, **131**(1):173-187.

CSA. 2012. Design and assessment of buildings subjected to blast loads. *CSA S850*. Mississauga, ON, Canadian Standards Association Group.

CSA. 2015. Qualification code for manufacturers of structural glued-laminated timber. *CSA O177*. Mississauga, ON, Canadian Standards Association Group.

Dorey, A.B., and Cheng, J.J.R. 1996a. The behavior of GFRP glued laminated timber beams. *Adv. Comp. Mat. in Bridges and Struct. II*, The Canadian Society for Civil Engineering, Montreal, Canada.

Dorey, A.B., and Cheng, J.J.R. 1996b. Glass Fiber Reinforced Glued Laminated Wood Beams. In *Canada-Alberta Agreement Documents*. Edmonton, Alberta: Natural Resources Canada, Canadian Forest Service, Northern Forestry Centre.

Hernandez, R., Davalos, J., F., Sonti, S.S., Kim, Y., and Moody, R., C. 1997. Strength and stiffness of reinforced yellow-poplar glued laminated beams. Madison, WI: U.S. Department of Agriculture, Forest Service, Forest Products Laboratory.

Johns, K.C., and Lacroix, S. 2000. Composite reinforcement of timber in bending. *Canadian Journal of Civil Engineering*, **27**(5):899-906.

Lacroix, D. 2017. Investigating the Behaviour of Glulam Beams and Columns Subjected to Simulated Blast Loading. Ph.D., Civil Engineering, University of Ottawa.

Sonti, S.S., GangaRao, H.V.S., and Superfesky, M.C. 1996. Rehabilitation and strengthening of glulam stringers for bridge superstructures. *First International Conference on Composites in Infrastructures*, University of Arizona, Tucson, Arizona.

Yang, H., Liu, W., Lu, W., Zhu, S., and Geng, Q. 2016. Flexural behavior of FRP and steel reinforced glulam beams: Experimental and theoretical evaluation. *Construction and Building Materials*, **106**:550-563.